

The effect of optical degradation from cataract using a new Deep Learning optical coherence tomography segmentation algorithm

*Original*

The effect of optical degradation from cataract using a new Deep Learning optical coherence tomography segmentation algorithm / Allegrini, Davide; Raimondi, Raffaele; Sorrentino, Tania; Tripepi, Domenico; Stradiotto, Elisa; Caruso, Marco; Paolo De Rosa, Francesco; Romano, Mario R.. - In: GRAEFE'S ARCHIVE FOR CLINICAL AND EXPERIMENTAL OPHTHALMOLOGY. - ISSN 0721-832X. - ELETTRONICO. - (2023). [10.1007/s00417-023-06261-4]

*Availability:*

This version is available at: 11583/2983105 since: 2023-10-18T13:18:56Z

*Publisher:*

Springer Nature

*Published*

DOI:10.1007/s00417-023-06261-4

*Terms of use:*

This article is made available under terms and conditions as specified in the corresponding bibliographic description in the repository

*Publisher copyright*

(Article begins on next page)



# The effect of optical degradation from cataract using a new Deep Learning optical coherence tomography segmentation algorithm

Davide Allegrini<sup>1</sup> · Raffaele Raimondi<sup>2</sup> · Tania Sorrentino<sup>2</sup> · Domenico Tripepi<sup>2</sup> · Elisa Stradiotto<sup>2</sup> · Marco Caruso<sup>3</sup> · Francesco Paolo De Rosa<sup>2</sup> · Mario R. Romano<sup>1,2</sup>

Received: 7 May 2022 / Revised: 25 September 2023 / Accepted: 28 September 2023  
© The Author(s), under exclusive licence to Springer-Verlag GmbH Germany, part of Springer Nature 2023

## Abstract

**Purpose** To assess the validity of the results of a freely available online Deep Learning segmentation tool and its sensitivity to noise introduced by cataract.

**Methods** The OCT images were collected with a Spectralis SD-OCT (Heidelberg Engineering, Heidelberg, Germany) as part of normal clinical practice. Data were segmented using a freely available online tool called Relayer (<https://www.relayer.online/>), based on a cross-platform Deep Learning segmentation architecture specifically adapted for retinal OCT images. The segmentations were read into MATLAB (The MathWorks, Natick, MA, USA) and analyzed.

**Results** There was an excellent agreement between the ETDRS measurements obtained from the two algorithms. Upon visual inspection, the segmentation based on Deep Learning obtained with Relayer appeared more accurate except in one case of apparent good quality image showing interrupted segmentations in some of the B-scans.

**Conclusion** A freely available online Deep Learning segmentation tool showed good and promising performance in healthy retinas before and after cataract surgery, proving robust to optical degradation of the image from media opacities.

**Keywords** Optical coherence tomography · OCT · Cataract optical degradation · Deep Learning · Segmentation algorithm

## Key messages

### What is known

- Deep learning algorithms are bringing artificial intelligence to clinical practice.
- There is lack of a coherence tomography segmentation algorithm free online tool

### What is new

- We tested a freely available online Deep Learning segmentation tool: the Relayer, which proved robust to optical degradation of the image from media opacity
- There was an excellent agreement between the ETDRS measurements obtained with Relayer and the Spectralis Heidelberg native algorithm.
- This online, free and reliable segmentation tool can help researchers using different OCT platforms to analyze with a uniform method their data.

✉ Raffaele Raimondi  
raffor9@gmail.com

<sup>1</sup> Eye Center, Humanitas Gavazzeni-Castelli, Bergamo, Italy

<sup>2</sup> Department of Biomedical Sciences, Humanitas University, Via Rita Levi Montalcini 4Pieve Emanuele, 20072 Milan, Italy

<sup>3</sup> PolitoBIOMed Lab—Biomedical Engineering Lab and Department of Electronics and Telecommunications, Politecnico Di Torino, 10129 Turin, Italy

## Introduction

Optical coherence tomography (OCT) is a non-invasive ocular imaging technology and an essential tool for the diagnosis and management of many eye diseases. This technology is employed for imaging of both the anterior and posterior segment of the eye and its applications have expanded exponentially thanks to improved image quality and analytical software tools. In posterior OCT, a segmentation of the different retinal layers is usually required for most clinical applications. Layer boundaries are often automatically detected by built-in software available with the machine. However, many platforms do not make segmentation data open to the user and this greatly limits research and clinical applications. Recent advancements in Deep Learning algorithms have greatly improved the accuracy of automated segmentation. However, Deep Learning algorithms need to be trained on large, labelled databases, often from one or few machines, and are usually not freely available for use by clinicians and researchers. Other platforms for segmentation have been made freely accessible but often require intensive computation which might not be achievable with the platforms available to the average user. Another issue is that the results of all segmentation algorithms are greatly influenced by image quality. Ocular media opacity, such as cataract, is one of the most common sources of noise in OCT images, often evident as a speckle pattern on the image and reduced contrast of layer boundaries [1].

The aim of our work was to assess the validity of the results of a freely available online Deep Learning segmentation tool and its sensitivity to noise introduced by cataract. We collected data from patients with clinically significant cataract and compared measurement results before and after surgery. The results were also compared with those made available by the OCT manufacturer, using a software tool validated for clinical use.

## Materials and methods

### Imaging data

The OCT images were collected with a Spectralis SD-OCT (Heidelberg Engineering, Heidelberg, Germany) as part of

normal clinical practice. The standard protocol at our clinic employs a  $30 \times 25$ -degree pattern with horizontal macular B-scans (61 B-scans) (9 averaged scans). Scans were visually inspected for patients with no evident retinal disease and who had a macular OCT scan performed within 1 month before and after uncomplicated cataract surgery. Macular volumes that contained clipped or partially obscured images within the central 10 degrees of the fovea were excluded. Because we wanted to analyze the effect of optical degradation from cataract on the segmentations of healthy retinas, we did not apply any selection based on signal strength and the only requirements were that the most reflective layers of the retina, the retinal nerve fiber layer (RNFL), and the retinal pigment epithelium (RPE) were fully visible within the images.

Data were exported as XML files, with the associated B-scans exported as individual TIFF files. Information about the scan, such as the pixel to mm conversion and the quality index (QI), was extracted from the XML file. The XML file also reported measurements about the full retinal thickness measured within the standard Early Treatment Diabetic Retinopathy Study (ETDRS) grid, with concentric rings of 1 mm, 3 mm, and 6 mm of diameter, with the two outermost rings divided into four sectors (i.e., Nasal, Superior, Temporal, Inferior).

### Data segmentation

Data were segmented using a freely available online tool called Relayer (<https://www.relayer.online/>), based on a cross-platform Deep Learning segmentation architecture specifically adapted for retinal OCT images (1). The website was accessed between February and March 2022. The images were uploaded onto the website and processed. The website provided segmentations of 11 retinal layers and the choroid (see example in Fig. 1) as individual CSV files (one for each B-scan) that could be downloaded and further analyzed.

### Data analysis

The segmentations were read into MATLAB (The MathWorks, Natick, MA, USA) and analyzed. Information from the XML file was used to create surfaces of all the segmented

**Fig. 1** Example of a segmentation result from Relayer, with our three-dimensional layer reconstruction, after flattening the Bruch's membrane

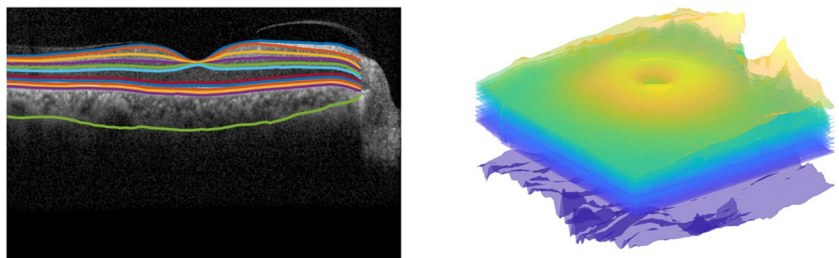
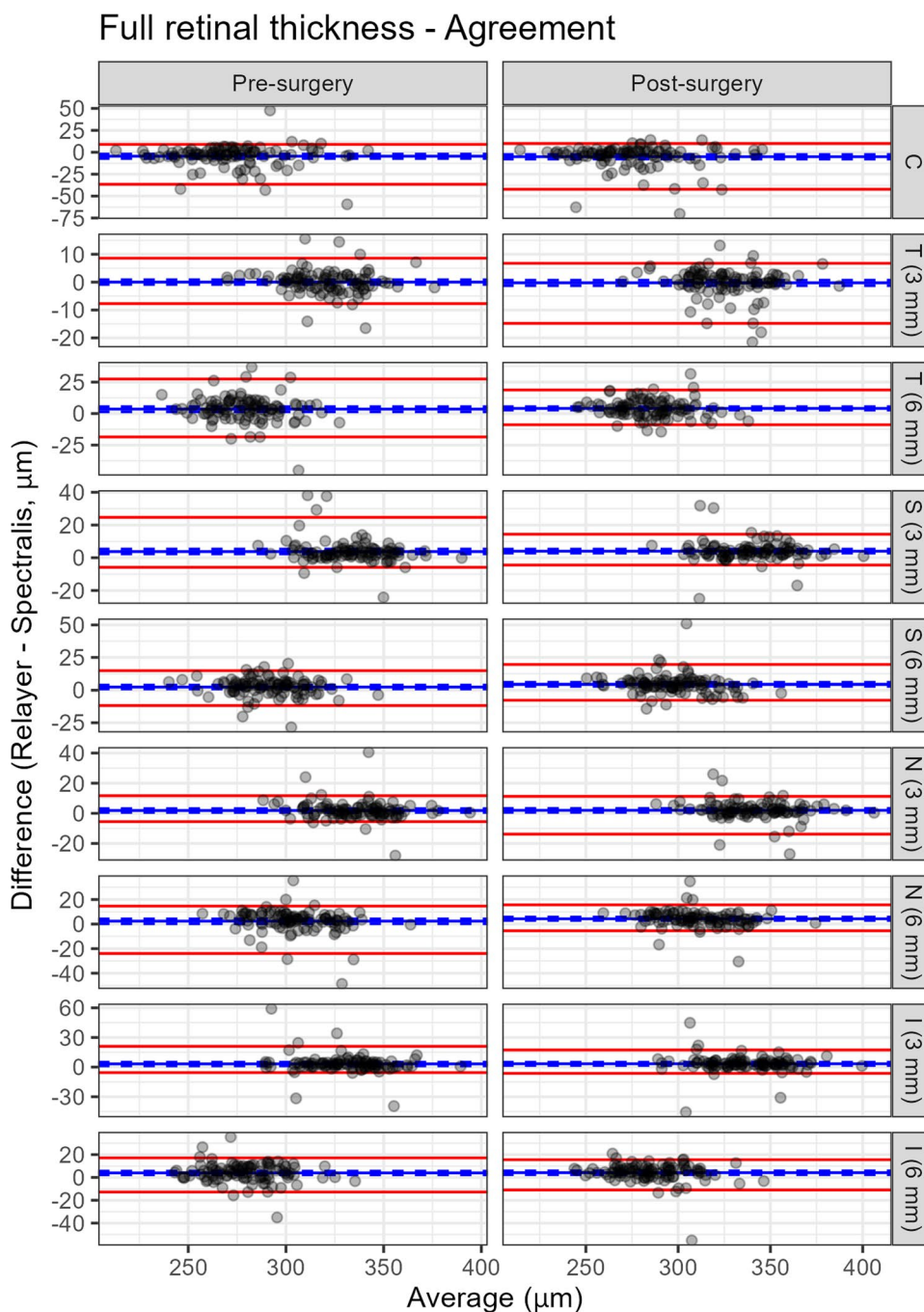


**Fig. 2** Bland–Altman analysis for the agreement between the pre- and post-operative measurements of the full retinal thickness for both algorithms. The solid lines represent the mean difference (blue, Post–Pre surgery) and the two limits of agreement (LoAs, red). The 95%-confidence intervals (CIs) are omitted for clarity. C, Central; N, Nasal; S, Superior; T, Temporal



layers and thickness maps for the full retina (from the inner limiting membrane, ILM, to the Bruch’s membrane, BM), the RNFL, the ganglion cell layer (GCL), the inner plexiform layer (IPL), and the outer retina (from the external limiting membrane to the BM). The fovea was automatically detected using a template matching technique and used as the center of a standard ETDRS grid, the same used by the Spectralis. Average thickness values were computed in each sector and in the central ring for all the layers described above.

Bland–Altman (BA) plots (2) were used to quantify:

- the differences in the measurements of the full retinal thickness obtained from the XML file (Spectralis) and those derived from Relayer’s segmentations.
- the differences between measurements of the different layers for each ETDRS sector obtained from scans before and after surgery. This was done only with the full retinal thickness for the Spectralis.

BA methodology was used to quantify average differences, 95% Limits of Agreement (LoA-97.5% and LoA-2.5%), and the

**Table 1** Bland–Altman analysis for the agreement between Relayer and Spectralis for the measurements of the full retinal thickness. The estimates are reported as Value [95% Confidence Intervals]. ETDRS,Early Treatment Diabetic Retinopathy Study; C, Central; N, Nasal; S, Superior; T, Temporal; I, Inferior. Values are reported in  $\mu\text{m}$ 

	ETDRS	Mean difference ( $\mu\text{m}$ )	Limit of agreement-97.5% ( $\mu\text{m}$ )	Limit of agreement-2.5% ( $\mu\text{m}$ )
Pre-surgery	C	-4.49 [-7.10, -2.06]	9.01 [5.98, 30.75]	-36.51 [-51.66, -22.82]
	N (3 mm)	0.01 [-0.83, 0.85]	8.59 [4.05, 15.03]	-7.71 [-15.35, -4.63]
	N (6 mm)	3.55 [1.44, 5.45]	27.45 [14.91, 33.24]	-18.54 [-33.20, -7.68]
	S (3 mm)	3.77 [2.36, 5.30]	24.70 [10.42, 37.91]	-5.85 [-17.17, -2.09]
	S (6 mm)	2.43 [1.00, 3.72]	14.82 [11.12, 19.02]	-11.78 [-24.59, -7.07]
	T (3 mm)	1.88 [0.61, 3.11]	11.67 [7.89, 32.73]	-5.53 [-19.68, -3.38]
	T (6 mm)	2.42 [0.34, 4.25]	14.65 [10.16, 35.53]	-23.94 [-39.25, -7.65]
	I (3 mm)	3.26 [1.27, 4.98]	21.03 [9.78, 47.26]	-5.57 [-35.77, -2.38]
	I (6 mm)	3.98 [2.29, 5.54]	17.14 [12.34, 31.23]	-12.76 [-25.88, -6.74]
Post-surgery	C	-5.07 [-7.73, -2.59]	9.94 [5.54, 13.92]	-42.21 [-66.71, -25.25]
	N (3 mm)	-0.24 [-1.26, 0.68]	6.76 [4.86, 11.38]	-14.78 [-19.84, -7.85]
	N (6 mm)	4.09 [2.73, 5.43]	18.72 [14.90, 31.50]	-8.87 [-13.96, -5.93]
	S (3 mm)	4.01 [2.83, 5.27]	14.38 [10.97, 31.14]	-4.45 [-21.18, -0.98]
	S (6 mm)	4.41 [2.97, 5.88]	19.58 [12.08, 37.79]	-7.69 [-12.73, -5.13]
	T (3 mm)	2.00 [0.67, 3.25]	11.27 [8.56, 23.93]	-13.80 [-24.18, -2.88]
	T (6 mm)	4.30 [3.01, 5.74]	15.67 [10.18, 34.79]	-5.44 [-23.97, -2.74]
	I (3 mm)	3.38 [1.67, 4.96]	17.34 [9.49, 33.94]	-6.33 [-38.68, -1.56]
	I (6 mm)	4.17 [2.44, 5.73]	15.52 [12.43, 18.99]	-10.98 [-35.39, -3.18]

corresponding 95% confidence intervals (95%-Cis). Note that we use the term limits of “agreement” instead of “repeatability” even for scan repeats, because the two scans were performed, by design, under different conditions and are not actually test–retest pairs. In addition, to compare the total spread of the differences between two test repeats (pre- and post-surgery) with the two full retinal segmentations (Spectralis and Relayer), we also quantified the range of the 95%-LoAs, i.e., the difference between the LoA-97.5% and the LoA-2.5%. Larger range indicates larger variability. All 95%-CIs and *p*-values were obtained through a paired bootstrap procedure (1000 samples), where the eye was the unit of resampling. This is particularly important to account for the paired nature of the data when comparing the segmentations from the Spectralis and Relayer. All statistical analyses were performed in R (R Foundation for Statistical Computing, Vienna).

## Results

### Cohort

We retrieved images from 98 healthy patients that underwent uncomplicated cataract surgery.

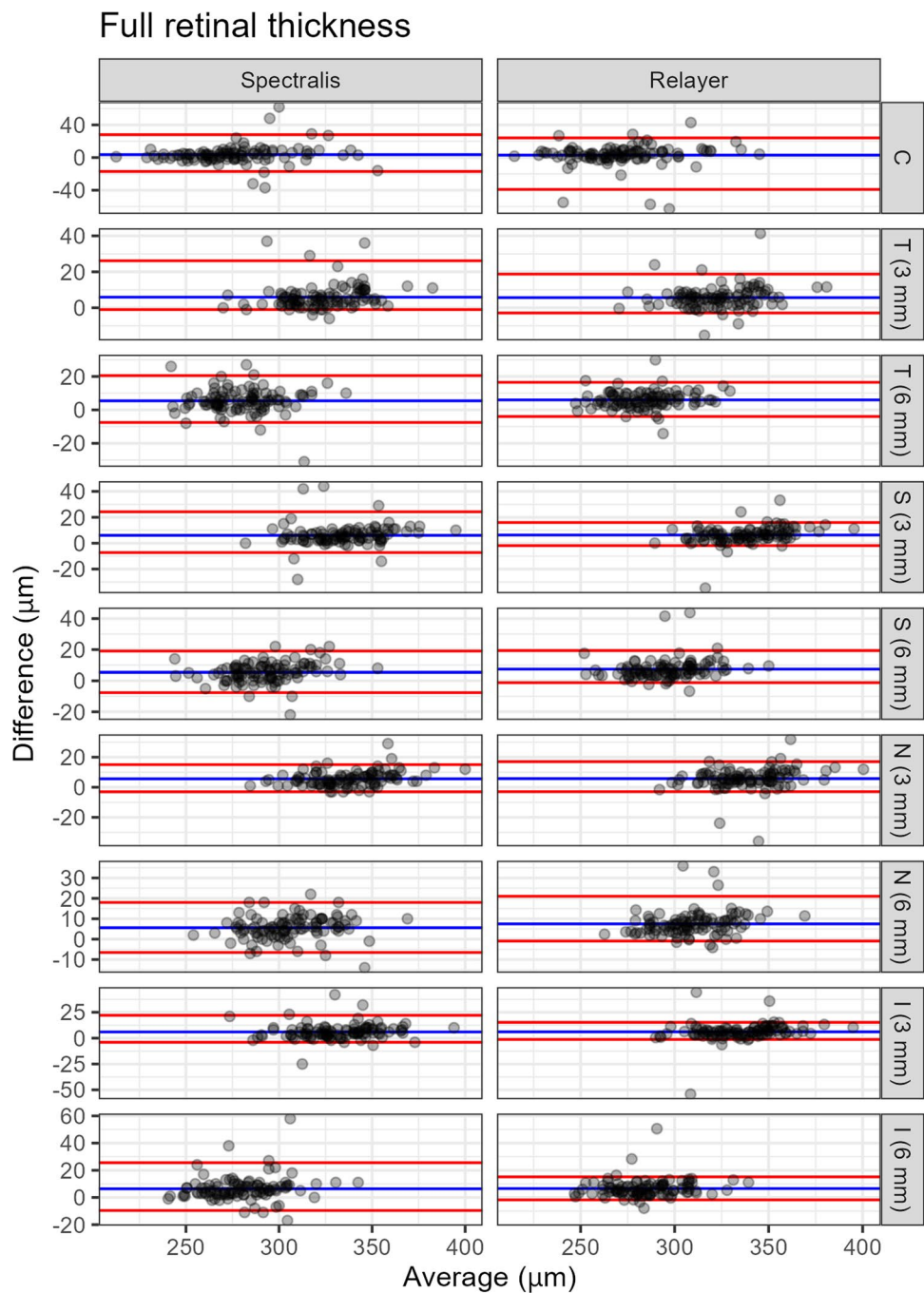
### Agreement

There was an excellent agreement between the ETDRS measurements obtained from the two algorithms (Pearson's correlation coefficient 0.96 both pre- and post-cataract surgery). The results of the BA analysis are reported in Fig. 2 and Table 1. In general, Relayer tended to measure thicker values, but the differences were small. We investigated the 9 scans where we found a disagreement of more than 20  $\mu\text{m}$ . These were mostly cases with a high amount of noise. Upon visual inspection, the segmentation based on Deep Learning obtained with Relayer appeared more accurate except in one case of apparent good quality image showing interrupted segmentations in some of the B-scans.

### Pre- and post-surgery comparison

Both algorithms measured thicker values for the full retinal thickness in the post-operative scans (Fig. 3 and Table 2). The average change in measured thickness was very similar between the two algorithms, with only occasionally significant small differences (Table 3).

**Fig. 3** Bland–Altman analysis for the agreement between Relayer and Spectralis for the measurements of the full retinal thickness. The solid lines represent the mean difference (blue, Relayer – Spectralis) and the two limits of agreement (LoAs, red). The dashed lines represent the 95%-confidence intervals (CIs) for the mean difference. The CIs for the LoAs are omitted for clarity. C, Central; N, Nasal; S, Superior; T, Temporal; I, Inferior



A similar trend was noted for the measurements obtained for the other retinal layers using Relayer, with generally larger values measured in the post-operative scans, as indicated by the positive difference from the BA analysis (Figs. 4 and 5 and Tables 3 and 4). The

same data are reported as percentage change from the mean in a Supplementary table, so that the LoAs of different layers can be compared directly. The most variable measurements were obtained for the outer retina and the choroid.

**Table 2** Bland–Altman analysis for the agreement between the pre- and post-operative measurements of the full retinal thickness for both algorithms. The estimates are reported as Value [95% Confidence Intervals]. ETDRS, Early Treatment Diabetic Retinopathy Study; C, Central; N, Nasal; S, Superior; T, Temporal; I, Inferior

		Spectralis	Relayer	<i>p</i>	
Mean difference (µm)	C	3.58 [1.39, 5.78]	3.01 [0.46, 5.23]	0.707	
	N (3 mm)	5.91 [4.71, 7.21]	5.65 [4.44, 6.97]	0.589	
	N (6 mm)	5.43 [3.96, 6.79]	5.97 [5.02, 6.94]	0.444	
	S (3 mm)	6.05 [4.41, 7.60]	6.29 [4.83, 7.59]	0.773	
	S (6 mm)	5.39 [4.05, 6.62]	7.37 [6.23, 8.78]	0.012	
	T (3 mm)	5.62 [4.70, 6.50]	5.74 [4.33, 7.05]	0.840	
	T (6 mm)	5.60 [4.48, 6.69]	7.48 [6.39, 8.68]	<b>0.011</b>	
	I (3 mm)	5.98 [4.47, 7.39]	6.10 [4.21, 7.78]	0.900	
	I (6 mm)	6.37 [4.85, 8.32]	6.56 [5.41, 7.86]	0.832	
	Limit of agreement 97.5% (µm)	C	28.05 [12.52, 55.35]	24.12 [16.04, 36.04]	0.736
		N (3 mm)	26.15 [13.00, 36.52]	18.74 [12.63, 33.09]	0.156
		N (6 mm)	20.52 [14.57, 26.52]	16.49 [11.67, 24.03]	0.219
		S (3 mm)	24.25 [13.00, 43.05]	15.99 [13.24, 28.91]	0.442
		S (6 mm)	19.05 [14.00, 22.00]	19.35 [13.13, 42.78]	0.998
T (3 mm)		15.05 [12.53, 24.25]	17.03 [13.09, 25.79]	0.112	
T (6 mm)		18.00 [12.00, 20.10]	21.03 [13.47, 34.58]	0.739	
I (3 mm)		22.05 [13.62, 37.25]	15.25 [12.54, 40.31]	0.359	
I (6 mm)		25.57 [16.10, 48.50]	15.15 [12.88, 40.01]	0.252	
Limit of agreement 2.5% (µm)		C	−17.05 [−34.62, −4.99]	−39.03 [−60.23, −7.83]	0.393
		N (3 mm)	−1.00 [−5.05, −0.51]	−2.88 [−12.25, −0.81]	0.566
		N (6 mm)	−7.53 [−21.98, −2.53]	−3.95 [−9.98, −0.37]	0.382
		S (3 mm)	−7.25 [−21.35, −0.99]	−1.89 [−21.41, 0.19]	0.482
		S (6 mm)	−7.62 [−16.30, −3.00]	−1.19 [−4.64, 1.69]	0.111
	T (3 mm)	−3.00 [−3.00, 0.00]	−2.93 [−30.20, −1.02]	1.000	
	T (6 mm)	−6.52 [−11.15, −2.53]	−0.93 [−3.44, 0.69]	<b>0.047</b>	
	I (3 mm)	−4.00 [−16.45, −1.05]	−1.30 [−31.44, 0.59]	0.519	
	I (6 mm)	−9.57 [−14.15, −2.00]	−1.78 [−5.75, 0.85]	<b>0.036</b>	
	Agreement range (µm)	C	45.10 [26.25, 78.37]	63.16 [28.54, 91.40]	0.514
		N (3 mm)	27.15 [14.00, 39.10]	21.62 [14.80, 39.55]	0.477
		N (6 mm)	28.05 [19.62, 45.60]	20.44 [13.93, 29.36]	0.190
		S (3 mm)	31.50 [15.05, 57.00]	17.88 [14.28, 45.63]	0.305
		S (6 mm)	26.67 [18.53, 37.35]	20.53 [14.00, 45.05]	0.545
T (3 mm)		18.05 [14.00, 27.25]	19.96 [14.99, 48.64]	0.981	
T (6 mm)		24.52 [17.57, 29.15]	21.96 [13.44, 36.09]	0.783	
I (3 mm)		26.05 [17.53, 46.00]	16.55 [13.62, 67.24]	0.360	
I (6 mm)		35.15 [23.15, 59.50]	16.93 [13.28, 42.66]	0.096	

Statistically significant *p* values in bold

## Discussion

This study assessed a freely available online Deep Learning OCT segmentation algorithm, Relayer, on healthy retinas of patients undergoing cataract surgery with the aim to evaluate the effect of cataract-related optical degradation on segmentation accuracy. Overall, the algorithm demonstrated a good performance on the tested sample. In particular, there was

an excellent agreement (0.96) between the ETDRS measurements obtained with Relayer and the Spectralis native algorithm. Both algorithms measured thicker values for the full retinal thickness in the post-operative scans (Fig. 3). The outer retina and choroid showed the largest percentage variability (Fig. 5).

Relayer is a freely online available segmentation tool that can facilitate access to quantitative OCT measurements,

**Table 3** Bland–Altman analysis for the agreement between the pre- and post-operative measurements of the inner retinal layers for Relayer. The estimates are reported as Value [95% Confidence Intervals]. *ETDRS*, Early Treatment Diabetic Retinopathy Study; *C*, Central; *N*, Nasal; *S*, Superior; *T*, Temporal; *I*, Inferior. *RNFL*, retinal nerve fiber layer; *GCL*, ganglion cell layer; *IPL*, inner plexiform layer

		Mean difference	Limit of agreement-97.5%	Limit of agreement-2.5%	
Full retina ( $\mu\text{m}$ )	C	3.01 [0.46, 5.23]	24.12 [16.04, 36.04]	-39.03 [-60.23, -7.83]	
	N (3 mm)	5.65 [4.44, 6.97]	18.74 [12.63, 33.09]	-2.88 [-12.25, -0.81]	
	N (6 mm)	5.97 [5.02, 6.94]	16.49 [11.67, 24.03]	-3.95 [-9.98, -0.37]	
	S (3 mm)	6.29 [4.83, 7.59]	15.99 [13.24, 28.91]	-1.89 [-21.41, 0.19]	
	S (6 mm)	7.37 [6.23, 8.78]	19.35 [13.13, 42.78]	-1.19 [-4.64, 1.69]	
	T (3 mm)	5.74 [4.33, 7.05]	17.03 [13.09, 25.79]	-2.93 [-30.20, -1.02]	
	T (6 mm)	7.48 [6.39, 8.68]	21.03 [13.47, 34.58]	-0.93 [-3.44, 0.69]	
	I (3 mm)	6.10 [4.21, 7.78]	15.25 [12.54, 40.31]	-1.30 [-31.44, 0.59]	
	I (6 mm)	6.56 [5.41, 7.86]	15.15 [12.88, 40.01]	-1.78 [-5.75, 0.85]	
	RNFL ( $\mu\text{m}$ )	C	-0.44 [-3.34, 1.85]	4.43 [3.23, 30.91]	-3.73 [-91.27, -1.38]
		N (3 mm)	-0.14 [-1.57, 1.04]	3.75 [3.19, 15.29]	-5.97 [-45.03, -2.96]
		N (6 mm)	0.89 [0.19, 1.45]	4.99 [3.46, 6.00]	-3.17 [-20.21, -1.20]
		S (3 mm)	0.49 [-1.46, 1.87]	6.89 [5.10, 15.82]	-8.48 [-57.53, -1.87]
		S (6 mm)	2.69 [1.79, 3.38]	7.95 [6.24, 10.15]	-3.19 [-20.73, -0.12]
T (3 mm)		-0.23 [-3.81, 2.71]	4.72 [3.77, 46.29]	-6.41 [-108.28, -2.72]	
T (6 mm)		3.49 [1.53, 5.60]	8.64 [8.06, 44.41]	-2.66 [-37.86, -0.93]	
I (3 mm)		1.05 [-0.64, 2.68]	6.83 [4.70, 29.03]	-3.30 [-49.06, -1.21]	
GCL ( $\mu\text{m}$ )	I (6 mm)	3.33 [2.49, 4.53]	9.23 [7.33, 29.90]	-1.89 [-8.83, -0.11]	
	C	0.89 [0.46, 1.44]	5.02 [3.19, 12.86]	-2.53 [-7.79, -1.15]	
	N (3 mm)	1.78 [1.31, 2.27]	7.88 [4.30, 11.89]	-2.47 [-5.89, -0.59]	
	N (6 mm)	1.39 [1.13, 1.65]	4.13 [3.45, 4.77]	-0.88 [-1.70, -0.56]	
	S (3 mm)	1.91 [1.20, 2.66]	4.91 [3.87, 23.31]	-1.18 [-9.35, -0.40]	
	S (6 mm)	1.02 [0.72, 1.31]	4.03 [2.63, 8.97]	-0.99 [-2.71, -0.39]	
	T (3 mm)	2.00 [1.07, 2.96]	7.50 [4.77, 28.98]	-2.32 [-14.97, -0.74]	
	T (6 mm)	1.13 [0.67, 1.64]	3.38 [2.80, 14.17]	-0.92 [-8.10, -0.25]	
IPL ( $\mu\text{m}$ )	I (3 mm)	1.71 [0.78, 2.65]	5.28 [4.05, 24.26]	-2.12 [-15.58, -0.67]	
	I (6 mm)	0.76 [0.35, 1.10]	3.52 [2.42, 7.23]	-1.35 [-8.38, -0.79]	
	C	0.38 [0.10, 0.69]	3.51 [2.16, 5.06]	-1.77 [-3.76, -1.34]	
	N (3 mm)	1.08 [0.54, 1.68]	6.02 [3.11, 16.56]	-3.22 [-7.58, -0.87]	
	N (6 mm)	0.99 [0.71, 1.28]	4.69 [2.94, 6.82]	-1.29 [-2.72, -0.66]	
	S (3 mm)	1.00 [0.47, 1.59]	3.52 [2.51, 17.29]	-1.66 [-7.76, -0.62]	
	S (6 mm)	0.70 [0.43, 0.98]	3.47 [2.38, 7.18]	-1.37 [-3.03, -0.77]	
	T (3 mm)	1.36 [0.55, 2.14]	5.63 [3.78, 23.02]	-1.72 [-12.39, -1.20]	
	T (6 mm)	0.63 [0.24, 1.02]	3.73 [2.23, 10.23]	-1.72 [-5.59, -1.04]	
	I (3 mm)	0.91 [0.13, 1.62]	4.62 [3.09, 19.44]	-2.41 [-13.05, -1.25]	
	I (6 mm)	0.55 [0.19, 0.85]	3.11 [2.58, 5.74]	-2.16 [-7.16, -0.46]	

especially for researchers. Indeed, we reported an excellent agreement with measurements obtained from clinical software, at least in healthy subjects. Moreover, Relayer seems robust to optical noise introduced by cataract; in fact, we reported a LoA range similar to Spectralis' segmentation software.

Both algorithms showed an increase in measured thickness in the post-operative scans (Fig. 2 and Table 2). This

change in thickness was very similar between the two algorithms and it likely originates from the image itself. This change may be attributed to different factors. One hypothesis is that the noise or other optical interference from cataract might have systematically altered the image, reducing the precision of both algorithms. However, we feel the most likely explanation is that the pixel to micron conversion in the Spectralis, reported in the XML file, was based on the



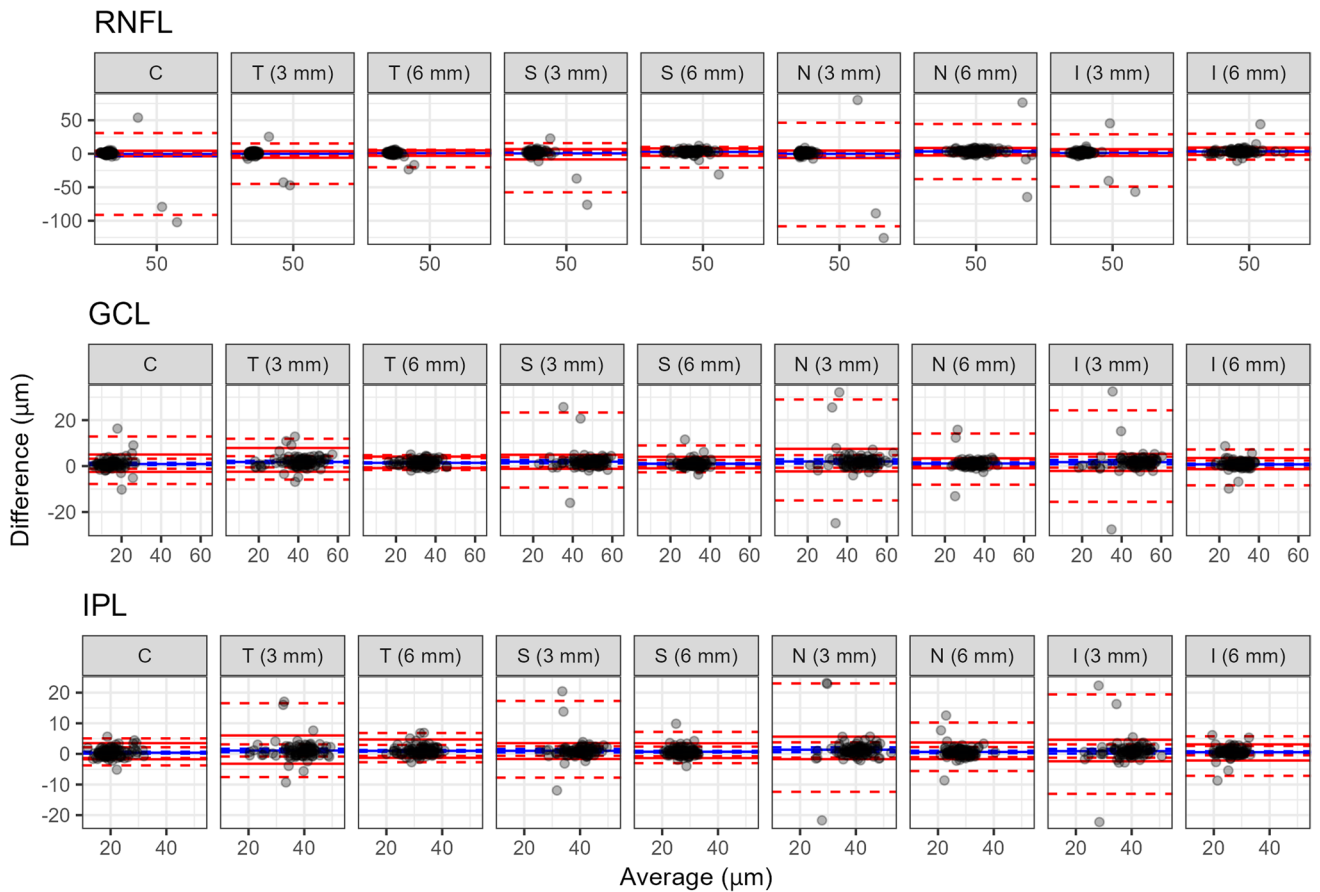


**Fig. 4** Bland–Altman analysis for the agreement between the pre- and post-operative measurements of the inner retinal layers. The solid lines represent the mean difference (blue, Post–Pre surgery) and the two limits of agreement (LoAs, red). The 95%-confidence Intervals

(CIs) are reported as dashed lines. C, Central; N, Nasal; S, Superior; T, Temporal; I, Inferior; RNFL, retinal nerve fiber layer; GCL, ganglion cell layer; IPL, inner plexiform layer

manual focus set by the user. This is linked to refraction in an attempt at correcting for ocular magnification. Moreover, another possibility is that the increase in thickness could be a genuine change due to low level surgically induced inflammation. We used the same scaling to be able to compare Relayer's measurements with those from the Spectralis. However, this is known to be somewhat inaccurate. (3) Moreover, because refraction was brought close to plano in all cases in this dataset, this operation might have introduced a systematic bias in the scaling of the ETDRS rings, which are defined in mm. At the same time, changes in the manual focus can also optically alter the lateral resolution of the scan. However, our findings are in accordance with van Velthoven et al. which reported that macular thickness measurements are slightly increased postoperatively [2].

The outer retina and choroid showed the largest percentage variability. This is somewhat expected because the layers in the outer retina are collectively very thin and a small variation can cause large proportional change. The choroid is notoriously difficult to measure, and these scans were not

specifically captured to highlight this structure, for example, by the use of Enhanced Depth Imaging.

A freely available online segmentation platform also allows the possibility to use the same algorithm for images captured from different devices and by different centers. This could provide a shared and standardized method of analyzing data for example in multicenter clinical studies reducing. Validating such applications will be the objective of future studies. Of notice, there are other freely available segmentation software tools, notably The Iowa Reference Algorithms (Retinal Image Analysis Lab, Iowa Institute for Biomedical Imaging, Iowa City, IA) (4), OCTMarker, an integrated free software package capable of segmenting approximately 2 or 3 retinal layers [3], Livelayer, a semi-automatic free software designed for segmentation of retinal layers and fluids [4], and the Orion platform. The latter has also been compared to the proprietary software such as the Spectralis in normal and pathologic eyes, with moderate-strong correlation [5]. Unlike these examples, however, Relayer is an online platform and does not require installation of software and the image processing is performed

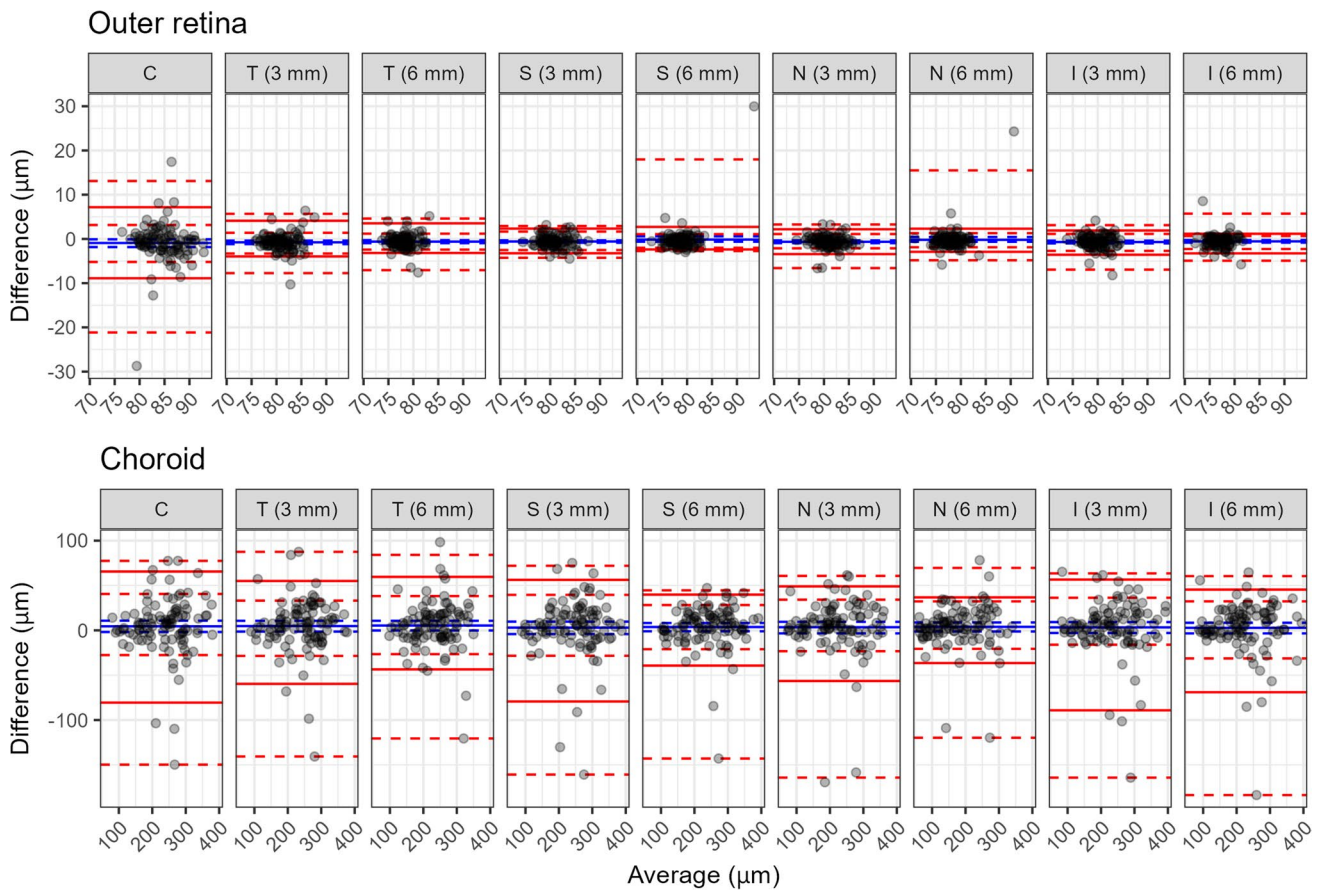


**Fig. 5** Bland–Altman analysis for the agreement between the pre- and post-operative measurements of the outer retina and the choroid. The solid lines represent the mean difference (blue, Post–Pre surgery)

and the two limits of agreement (LoAs, red). The 95%-confidence Intervals (CIs) are reported as dashed lines. C, Central; N, Nasal; S, Superior; T, Temporal; I, Inferior

**Table 4** Bland–Altman analysis for the agreement between the pre- and post-operative measurements of the outer retina and choroid for Relayer. The estimates are reported as Value [95% Confidence Inter-

vals]. *ETDRS*, Early Treatment Diabetic Retinopathy Study; C, Central; N, Nasal; S, Superior; T, Temporal; I, Inferior

		Mean difference	Limit of agreement-97.5%	Limit of agreement-2.5%
Outer retina (µm)	C	-0.92 [-1.84, -0.09]	7.17 [3.15, 13.10]	-8.89 [-21.15, -5.20]
	N (3 mm)	-0.76 [-1.18, -0.38]	4.11 [1.39, 5.68]	-3.96 [-7.73, -3.30]
	N (6 mm)	-0.61 [-0.95, -0.28]	3.53 [1.19, 4.61]	-3.17 [-7.06, -2.42]
	S (3 mm)	-0.58 [-0.86, -0.31]	2.34 [1.66, 2.93]	-3.24 [-4.26, -2.51]
	S (6 mm)	-0.15 [-0.62, 0.59]	2.72 [1.09, 17.98]	-2.38 [-2.74, -2.00]
	T (3 mm)	-0.65 [-0.95, -0.34]	2.18 [1.11, 3.26]	-3.43 [-6.59, -2.11]
	T (6 mm)	-0.20 [-0.65, 0.44]	2.31 [1.29, 15.50]	-2.92 [-4.82, -1.89]
	I (3 mm)	-0.70 [-1.01, -0.39]	1.90 [1.14, 3.12]	-3.58 [-6.94, -2.70]
	I (6 mm)	-0.55 [-0.84, -0.25]	1.17 [0.66, 5.72]	-3.26 [-4.93, -2.28]
	Choroid (µm)	C	4.47 [-1.85, 10.75]	65.59 [40.56, 77.45]
N (3 mm)		4.74 [-1.40, 10.63]	55.03 [33.12, 87.51]	-59.68 [-140.64, -28.51]
N (6 mm)		5.37 [-0.16, 10.66]	59.60 [38.22, 84.15]	-43.53 [-120.55, -26.55]
S (3 mm)		3.03 [-4.16, 9.70]	56.29 [39.55, 71.97]	-79.33 [-160.79, -28.35]
S (6 mm)		3.70 [-1.07, 8.17]	39.82 [28.22, 44.60]	-39.31 [-142.90, -21.04]
T (3 mm)		3.48 [-3.39, 9.49]	49.02 [34.20, 60.69]	-56.49 [-164.15, -23.26]
T (6 mm)		3.86 [-1.26, 8.77]	36.75 [32.28, 69.61]	-36.49 [-119.72, -20.62]
I (3 mm)		3.30 [-2.95, 9.21]	56.60 [36.30, 63.50]	-89.15 [-164.20, -16.05]
I (6 mm)		2.81 [-3.41, 8.45]	45.41 [32.33, 60.44]	-68.99 [-183.64, -31.31]

online. This is potentially beneficial, as it would not require intensive computation on the user's machine and can be used with different operating systems and devices.

The limitations of this study include the limited sample size, the inclusion of healthy eyes only, and the fact that a comparison with the Spectralis' native segmentation was only performed for the full retinal thickness. Further investigation is required to evaluate how the algorithm performs in retinas altered by disease eyes, such as macular edema or macular epiretinal membranes.

## Conclusions

A freely available online Deep Learning segmentation tool showed good performance in healthy retinas before and after cataract surgery, proving robust to optical degradation of the image from media opacities.

## References

1. Schmitt JM, Xiang SH, Yung KM (1999) Speckle in optical coherence tomography. *J Biomed Opt* 4:95–105. <https://doi.org/10.1117/1.429925>
2. van Velthoven MEJ, van der Linden MH, de Smet MD et al (2006) Influence of cataract on optical coherence tomography image quality and retinal thickness. *Br J Ophthalmol* 90:1259–1262. <https://doi.org/10.1136/bjo.2004.097022>
3. Motamedi S, Gawlik K, Ayadi N et al (2019) Normative data and minimally detectable change for inner retinal layer thicknesses using a semi-automated OCT image segmentation pipeline. *Front Neurol* 10:1117. <https://doi.org/10.3389/fneur.2019.01117>
4. Montazerin M, Sajjadifar Z, Khalili Pour E et al (2021) Livelayer: a semi-automatic software program for segmentation of layers and diabetic macular edema in optical coherence tomography images. *Sci Rep* 11:13794. <https://doi.org/10.1038/s41598-021-92713-y>
5. Alex V, Motevasseli T, Freeman WR et al (2021) Assessing the validity of a cross-platform retinal image segmentation tool in normal and diseased retina. *Sci Rep* 11:21784. <https://doi.org/10.1038/s41598-021-01105-9>

**Publisher's Note** Springer Nature remains neutral with regard to jurisdictional claims in published maps and institutional affiliations.

Springer Nature or its licensor (e.g. a society or other partner) holds exclusive rights to this article under a publishing agreement with the author(s) or other rightsholder(s); author self-archiving of the accepted manuscript version of this article is solely governed by the terms of such publishing agreement and applicable law.